IOP Publishing Phys. Med. Biol. 66 (2021) 085003 https://doi.org/10.1088/1361-6560/abe554

Physics in Medicine & Biology

IPEM Institute of Physics and Engineering in Medicine

OPEN ACCESS

RECEIVED
28 September 2020

REVISED
22 January 2021

ACCEPTED FOR PUBLICATION
11 February 2021

PUBLISHED
15 April 2021

PAPER

Al_2O_3:C optically stimulated luminescence dosimeters (OSLDs) for ultra-high dose rate proton dosimetry

Jeppe Brage Christensen[1], **Michele Togno**[2], **Konrad Pawel Nesteruk**[2], **Serena Psoroulas**[2], **David Meer**[2], **Damien Charles Weber**[2,3,4], **Tony Lomax**[2,5], **Eduardo G Yukihara**[1] **and Sairos Safai**[2]

[1] Department of Radiation Safety and Security, Paul Scherrer Institute, Switzerland
[2] Center for Proton Therapy, Paul Scherrer Institute, Switzerland
[3] Department of Radiation Oncology, University Hospital Zurich, Switzerland
[4] Department of Radiation Oncology, University Hospital Bern, Switzerland
[5] Department of Physics, ETH Zurich, Switzerland

E-mail: eduardo.yukihara@psi.ch

Keywords: FLASH, proton dosimetry, optically stimulated luminescence, Al_2O_3:C, ultra-high dose rate

Supplementary material for this article is available online

Abstract

The response of Al_2O_3:C optically stimulated luminescence detectors (OSLDs) was investigated in a 250 MeV pencil proton beam. The OSLD response was mapped for a wide range of average dose rates up to 9000 Gy s^{-1}, corresponding to a ~150 kGy s^{-1} instantaneous dose rate in each pulse. Two setups for ultra-high dose rate (FLASH) experiments are presented, which enable OSLDs or biological samples to be irradiated in either water-filled vials or cylinders. The OSLDs were found to be dose rate independent for all dose rates, with an average deviation <1% relative to the nominal dose for average dose rates of (1–1000) Gy s^{-1} when irradiated in the two setups. A third setup for irradiations in a 9000 Gy s^{-1} pencil beam is presented, where OSLDs are distributed in a 3 × 4 grid. Calculations of the signal averaging of the beam over the OSLDs were in agreement with the measured response at 9000 Gy s^{-1}. Furthermore, a new method was presented to extract the beam spot size of narrow pencil beams, which is in agreement within a standard deviation with results derived from radiochromic films. The Al_2O_3:C OSLDs were found applicable to support radiobiological experiments in proton beams at ultra-high dose rates.

1. Introduction

The use of radiotherapy with ultra-high dose rates (>40 Gy s^{-1}, termed FLASH) has been studied for decades (Hornsey and Alper 1966, Town 1967) with renewed interest in recent years (Favaudon *et al* 2014, Vozenin *et al* 2019, Bourhis *et al* 2019a, 2019b). Whilst studies with FLASH intense electron beams have been undertaken at clinical linear accelerators (Lempart *et al* 2019) or superconducting linear accelerators (Karsch *et al* 2012), less attention has been devoted to FLASH therapy with proton beams. Patriarca *et al* (2018) presented a setup for proton dose rates above 40 Gy s^{-1}, with Beyreuther *et al* (2019) and Diffenderfer *et al* (2020) using 100 Gy s^{-1} and 78 Gy s^{-1} proton beams, respectively, for irradiation of biological samples. Buonanno *et al* (2019) used 4.5 MeV protons to achieve a narrow beam with a dose rate of 1 kGy s^{-1}, and Darafsheh *et al* (2020) applied a synchrocyclotron to achieve (100–200) Gy s^{-1} dose rates for a 70 MeV beam. However, few experiments have been conducted, if any, for dose rates >1000 Gy s^{-1} in clinically relevant proton beams due to accelerator limitations (Esplen *et al* 2020). For proton pencil beams with energies above 200 MeV, the highest dose rate is generally achieved in the entrance regions before the beam undergoes scattering. For dosimetry in such beams to support radiobiological experiments, one needs a detector capable of measuring a dose delivered with ultra-high dose rates, and that can be placed in a water-filled container depending on the type of biological sample.

Whilst ionization chambers remain the golden standard in dosimetry, and despite a negligible amount of the initial recombination in air-filled ionization chambers, the general recombination exceeds correctable levels for proton beams at ultra-high dose rates (Christensen *et al* 2020a). Radiochromic films have been shown to be dose

rate independent in electron beams (Jaccard *et al* 2017) and for proton beams <200 Gy s^{-1} (Darafsheh *et al* 2020), but accurate dosimetry using radiochromic films is still challenging. Faraday cups (Gomà *et al* 2014) and absorbed dose calorimetry (Christensen *et al* 2020b) are available to integrate the dose with high accuracy, but inapplicable for measuring the dose under nominally same radiation conditions as a biological sample, in particular if the samples need to be contained in water.

Luminescence detectors can potentially provide the small size, accuracy, water-resistance, and dose rate independency required for dosimetry in vials with biological samples irradiated with FLASH intense proton beams. Optically stimulated luminescence (OSL), in particular, is now a technique widely used in personal dosimetry and well accepted in medical dosimetry (Akselrod *et al* 2007, Yukihara and McKeever 2008, Mijnheer *et al* 2013, Kry *et al* 2020), having been used for postal audits by various countries (Casey *et al* 2013, Lye *et al* 2014, Wesolowska *et al* 2017).

The OSL from Al_2O_3:C has been shown to provide the possibility of high-precision dosimetry (<1% per detector) when using the bare detectors read by automated research readers capable of irradiating the detectors in the reader, immediately after the readout. Hence, the signal from an experimental irradiation session can be compared directly to the signal from a reference irradiation, providing a normalization signal to compensate for variations in detector mass and sensitivity (Yukihara *et al* 2005). This means that small detectors can be prepared from the original commercial ones, allowing precise dosimetry of small fields. The material has also been characterized for dosimetry of proton and carbon ion beams used in radiation therapy and has been shown to provide information on the ionization density of the radiation field (Yukihara and McKeever 2006, Sawakuchi *et al* 2010, Yukihara *et al* 2015). A general overview of the properties of Al_2O_3:C OSL can be found in the report of the Task Group 191 of the American Association of Physicist in Medicine (Kry *et al* 2020).

Not much information is available on the dose rate dependence of OSL detectors (OSLDs), although its presence has been predicted theoretically for a simplified OSL model in limited conditions (Chen and Leung 2001a, 2001b). The dependence of Al_2O_3:C on dose rate has been experimentally investigated for the dose rates normally encountered in radiation therapy, but no significant dependence was found (Jursinic 2007). Another study looked at BeO at extremely high dose rates (0.2–2.8) $\times$ 10^9 Gy s^{-1} in electron beams (Karsch *et al* 2012) and also reported no significant dependence.

The objective of this work was to investigate the dose rate dependence of Al_2O_3:C OSLDs for proton beams with dose rates in the 1–9000 Gy s^{-1} range. The high dose rates were achieved using a single pencil beam, where the OSLDs were placed at the central beam axis of the beam. The final aim is to develop a setup with detectors to support future radiobiology experiments with ultra-high proton dose rates at the Paul Scherrer Institute (PSI) Proton Therapy Center.

2. Materials and methods

2.1. Beam size and dose rate definition

Single pencil beams were used for all experiments. The beam is quasi-continuous with the RF frequency of the COMET cyclotron being 72.85 MHz, so a pulse is delivered every 14 ns with each pulse being 0.8 ns. The dose rate within a pencil beam referred to in this work, if not otherwise specified, is an *average* value estimated from the proton beam current derived from the delivery time of each spot as measured by the control system and the number of delivered protons as measured with a Faraday cup. The accuracy of the delivered time is within 50 μs. The instantaneous dose rate within a pulse, according to the cyclotron frequency and pulse width, is about 17 times higher than the above estimated average dose rate. The combined uncertainties of the Faraday cup measurements, the beam spread, and the delivery time amounts to a dose rate uncertainty of 5%. The beam was degraded by means of range shifter plates for the (1–1000) Gy s^{-1} dose rates to scatter the beam and thus obtain a 4 mm diameter field with a maximum 5% deviation from the maximum dose at the central axis. The dose profile was verified independently with a scintillating screen and a CCD camera with a spot size variation less than 1% between irradiations, and was independent of the deposited dose. The dose rate was increased to 9000 Gy s^{-1} (~150 kGy s^{-1} instantaneous dose rate in each pulse) at the central beam axis by removing the range shifter plates, which in turn decreases the pencil beam spot size. A smaller beam size gives a smaller evaluated dose due to the signal averaging of the beam over the OSLD surface. Hence, when the dose rate is increased by decreasing the beam size, the measured central dose is underestimated when the averaging effect in a detector is not taken into account. This is a result of the signal averaging effect varying with the spot size, which needs to be distinguished from an actual dose rate effect of the OSLD response. The signal averaging is examined by integrating a two-dimensional Gaussian, approximating the experimentally relevant pencil beams, over the OSLD surface for a given beam spot center.

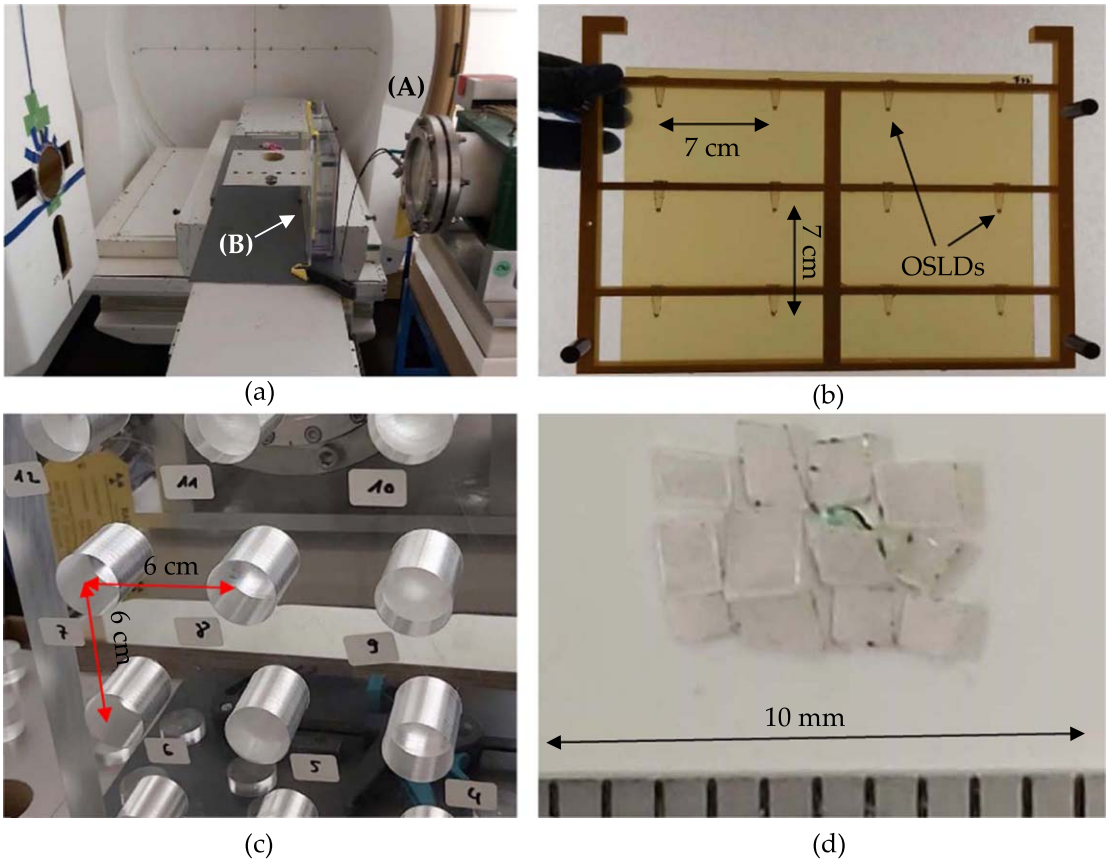

Figure 1. (a) The experimental setup with (A) the Faraday cup and (B) side-view of setup A. (b) Setup A where the 12 water-filled vials with OSLDs are visible at the bottom of each vial. (c) Setup B where the PMMA frame contains 12 cylinders. The OSLDs in the cylinders are not visible. (d) Setup C where 3 × 4 OSLDs are placed in a grid before being wrapped in opaque tape. The setup details and dimensions are given in the text.

2.2. Optically stimulated luminescence detectors

The OSLDs were prepared from the same type of detectors used in the Luxel^{TM} dosimetry system (Landauer), consisting of Al_2O_3:C powder mixed with a binder and enclosed within two polymer sheets (Akselrod *et al* 2000) forming a 0.3 mm thick detector film. The detector film is chemically stable and allows for irradiation in water. The original detectors were cut by hand to approximately 1 mm by 1 mm sizes from the same batch. The detectors were bleached using a green LED (525 nm) filtered by Schott GG495 filters (3 mm thickness) before use.

2.3. Experimental design

The experiments were carried out at Gantry 1 at PSI (Lin *et al* 2009) with a 250 MeV proton pencil beam (Nesteruk *et al* 2020). A Faraday cup (Gomà *et al* 2014) was placed behind the target as shown in figure 1(a) and used to measure the number of protons to verify the delivered dose. The OSLDs were irradiated in a blacked out room and placed in opaque packages after each irradiation for subsequent readout. The biological samples are to be stored in water and, therefore, the OSLDs were irradiated under similar conditions in identical water-filled containers. Two setups were tested to accommodate OSLDs or biological samples and a third only for OSLDs as described below.

2.3.1. Setup A: water-filled vials

A plastic frame was used to confine the 12 vials (0.2 ml PCR tubes, Eppendorf AG, Germany) as shown in figure 1(b). The frame was immersed in a water tank that also accommodates a radiochromic film (Gafchromic™ EBT3, Ashland, USA) visible in figure 1(b) behind the vials. The vials were filled with water and either OSLDs or biological samples were placed at the bottom of each vial. Five frames with 12 vials each and a single frame containing eight vials were irradiated with dose rates between (5–1000) Gy s^{-1} in this way. The pencil beam width for this setup was $\sigma_x = \sigma_y = 6.2$ mm, where x and y denote the horizontal and vertical directions, respectively.

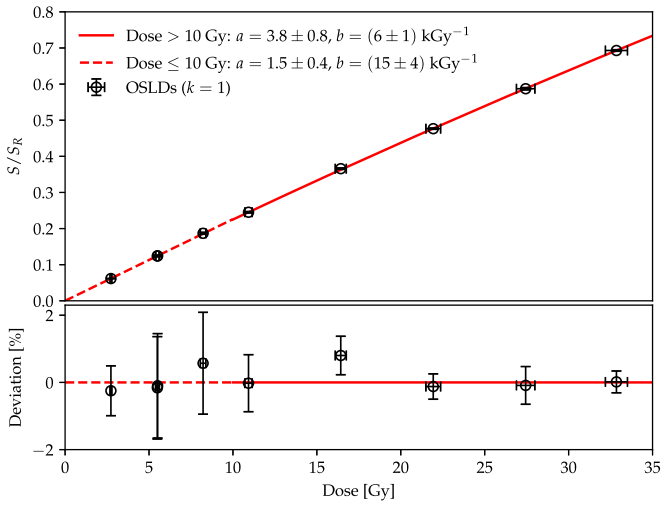

Figure 2. The ratio of the signal S from the experimental irradiation to the reference irradiation S_R as a function of the dose measured with an ionization chamber. Equation (1) is fitted separately to the data above and below 10 Gy. The lower figure shows the deviation of the data points to the fit. The 5.5 Gy irradiation was repeated to investigate the reproducibility.

2.3.2. Setup B: water-filled PMMA cylinders

A 5 cm thick PMMA plate, partly shown in figure 1(c), accommodates 12 cylinders of 2.5 cm diameter and 2.0 cm height. Each cylinder is placed in the frame with a 2.2 cm PMMA build-up in front and 0.8 cm PMMA behind. A 2.5 mm diameter hole was drilled through the cylinder axes, and each cylinder was filled with water to accommodate either OSLDs or biological samples. The pencil beam axis is centered over each cylinder axis, where an OSLD is placed at the front and back of the cylinder and two OSLDs float in the middle to reflect the dose variations to the biological samples. This setup was used for irradiations with the three pencil beams 1 Gy s^{-1} ($\sigma_x = \sigma_y = 5.0$ mm), 1400 Gy s^{-1} ($\sigma_x = \sigma_y = 5.0$ mm) and 3800 Gy s^{-1} ($\sigma_x = \sigma_y = 3.5$ mm).

2.3.3. Setup C: OSLDs in a 2D grid for narrow pencil beams

For the special case of the narrow 9000 Gy s^{-1} pencil beam ($\sigma_x = 2.3$ mm, $\sigma_y = 1.8$ mm), 12 OSLDs were aligned in a 3 × 4 grid as exemplified in figure 1(d). The 12 OSLDs were wrapped in opaque tape with a ∼1 mm thickness of the package. Six packages, each with OSLDs in a 3 × 4 grid, were irradiated with 9000 Gy s^{-1}, where the beam was approximately centered over the middle of each package. The OSLDs were read out individually post irradiation, and the 12 doses at known positions in each package were used to reconstruct the dose of the Gaussian beam, as well as the spot size and position of the center: the dose to each OSLD was calculated, given a certain spread, position, and dose of the beam, by averaging the Gaussian function over each OSLD. The dose, position, and beam spread which minimizes the sum of the squared differences between the measured and calculated doses was taken to be the best estimate of the true beam position over the OSLD grid, dose, and beam spread.

2.4. OSLD readout and calibration in a proton beam

The OSLDs were read out using the Risø reader (TL/OSL-DA-20, DTU Nutech, Denmark) using green light stimulation (525 nm, ∼40 mW cm^{-2}) and a photomultiplier tube (PMT; ET Enterprises PMD9107Q-AP-TTL) for light detection. A Hoya U-340 filter was used to block the stimulation light from reaching the PMT. An additional neutral density filter (Edmund Optics UV/VIS ND OD 2.0) was used to reduce the light intensity. The OSL was stimulated for 300 s and the total signal was integrated. The background signal was estimated using the last 10 data points of the OSL curve and subtracted, resulting in the net OSL signal S. The OSLD was subsequently subject to a reference irradiation of (1000 s) from a ^{90}Sr/^{90}Y beta source in the Risø reader, which, after the same readout procedure as above, gave a 'reference' signal S_R. The ratio of the signal S from the experimental irradiation to the reference irradiation S_R in the reader hence is a measure of the energy deposited in the OSLD during the experiment independent of the OSLD size. Nevertheless, the ratio S/S_R is also affected by sensitivity changes in the Al_2O_3:C and, therefore, a proper calibration curve must be determined (Yukihara *et al* 2005). The reference dose to the OSLDs, delivered by the source in the reader during the 1000 s irradiation, is irrelevant provided it remains constant for all reference irradiations. The reference dose may be derived from the calibration curve in section 3.1.1 to be ∼47 Gy.

For a calibration in a proton beam, the OSLDs were irradiated in groups of four together with an ionization chamber (Advanced Markus, PTW Freiburg, Germany) for a range of doses between 3 and 33 Gy at a clinically

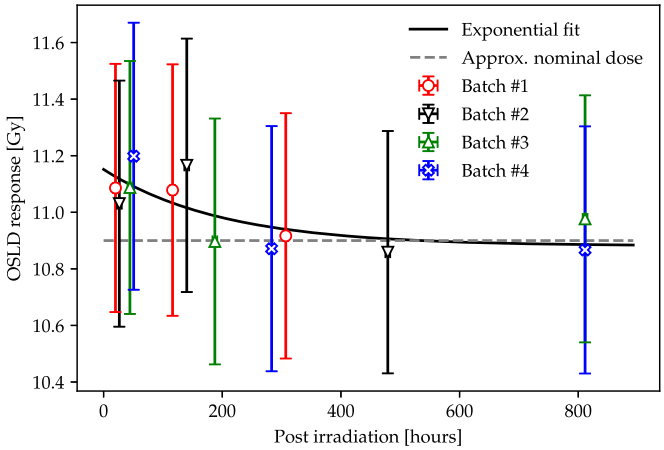

Figure 3. The OSLD response as a function of time. The dashed line denotes the dose delivered to the OSLDs and the solid line the exponential function fitted to all data points.

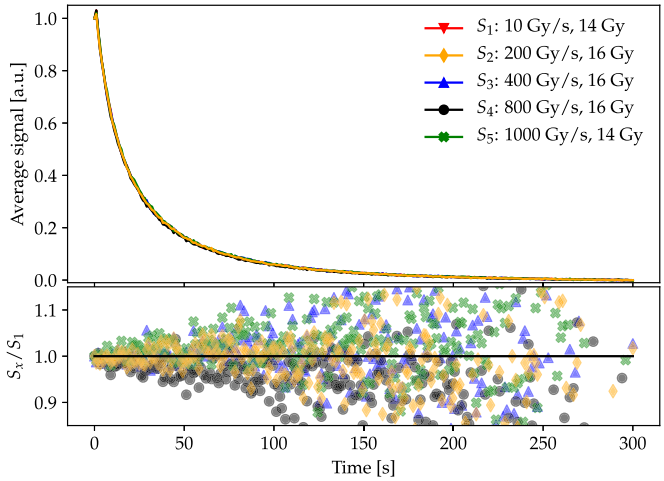

Figure 4. Each curve shows the average of four OSLD readout signals normalized to the entry, where the background signal has been subtracted. The lower scatter plot shows the ratio of each signal to the signal obtained from the irradiation with the lowest dose rate.

relevant dose rate up to 12 Gy s^{-1} in a 5.0 $\times$ 5.0 cm^2 field size. The mean S/S_R of the four OSLDs in each irradiation, plotted as a function of the dose measured with the ionization chamber, enables an interpolation and conversion of the OSLD signal ratio S/S_R to a dose provided it was irradiated in the calibration dose range.

3. Results and discussion

3.1. OSLD response

3.1.1. Proton calibration curve

The ratio of the signal S from the OSLD irradiated with protons to the signal from the reference irradiation S_R is in figure 2 plotted as a function of the irradiation dose measured with the ionization chamber as outlined in section 2.4. Each data point is the mean value of the S/S_R ratio for four OSLDs irradiated in the same session and plotted with ($k = 1$) statistical standard deviation error bars. A function of the form

$$\frac{S}{S_R}(D) = a(1 - \exp(-bD)) \tag{1}$$

is fitted to the data piecewise, above and below 10 Gy, respectively. Equation (1) fitted to the data above 10 Gy is plotted in figure 2 with a solid line, whereas the fit to the data below 10 Gy is shown with a dashed line. The fit parameters are given in the figure legend. The fit enables an interpolation of a measured S/S_R ratio to a dose in the calibration range. The 5.5 Gy irradiation was repeated to assess the reproducibility, which generally is of the order of 0.5%.

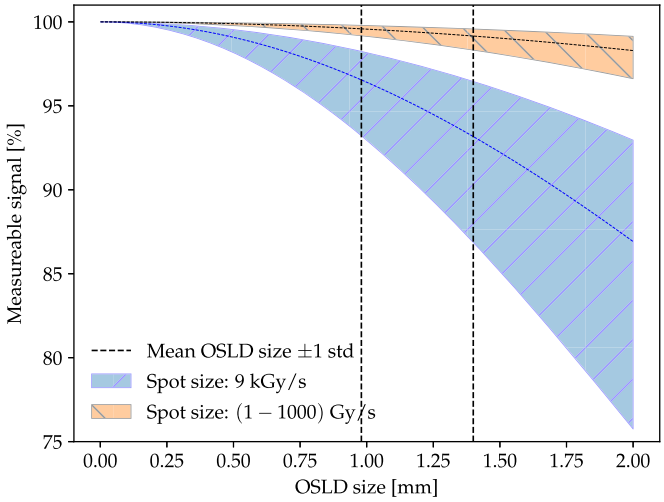

Figure 5. Achievable pencil beam measurements with OSLDs for two cases approximately corresponding to the (1–1000) Gy s^{-1} and 9000 Gy s^{-1} beams with the beam spot sizes given in the text. The hatched area shows the minimum and maximal measureable signal given the OSLD and beam size. The average measurable signals shown with dots for each spot size and the vertical dashed lines are explained in the text.

The parameters in equation (1) are obtained with the LMFIT package (Newville *et al* 2016) for python3.8. The reported uncertainty of any dose measured by an OSLD in this work is the combined statistical standard deviation ($k = 1$) of each group of OSLDs and the uncertainty derived from the calibration curve. As most of the OSLD doses are plotted relative to the dose derived from the Faraday cup measurement, another 4% uncertainty from the Faraday cup measurement (Gomà *et al* 2014, Winterhalter *et al* 2018) is added to the OSLD dose measurement. The combined uncertainty for a 10 Gy dose measurement with a single OSLD typically amounts to 6%.

3.1.2. OSLD fading

The fading of the OSLD signal after the irradiation was examined by irradiating 12 packages with four OSLDs each. The packages were irradiated with 10.9 Gy 210 MeV protons over four runs, with three packages each, to minimize any perturbation of the beam. The packages were read out over the course of a few weeks with the results, after converting the S/S_R signal to a dose, plotted in figure 3. The variation of the data points with time is approximated with an exponential function, as shown in the figure, which however does not fully account for the data behavior. The exponential fit is hence regarded as an estimate of the fading of the OSLDs. The OSLDs, irradiated during the experiments, were readout between 48 and 510 h after the irradiation and subject to a fading correction below 1.8%.

3.1.3. Luminescence signal for different dose rates

The OSL signal is plotted as a function of stimulation time in figure 4 for several dose rates. Each curve is the mean of four OSL readout for the same dose rates, where the background (around 1% relative to the maximum luminescence for a 10 Gy irradiation) has been subtracted and the curve normalized to the entrance value. The ratio of each of the curves to the signal obtained with the lowest dose rate ($S_1 = 10$ Gy s^{-1}) is shown below.

The fact that the OSL curves for dose rates between 10 and 1000 Gy s^{-1} all coincide (figure 4) suggests that no change in the ionization and trapping processes related to the production of OSL occurs with the dose rate, as opposed to what has been observed for various ionization densities (Yukihara and McKeever 2006, Sawakuchi *et al* 2010).

3.1.4. Signal averaging in pencil beams

The effect of averaging a pencil beam over the OSLD is mapped in figure 5 for different beam and OSLD sizes. The pencil beams for dose rates (1–1000) Gy s^{-1} are approximated with a Gaussian function with $\sigma_x = \sigma_y = 6.2$ mm. The 9000 Gy s^{-1} beam is modeled with $\sigma_x = 2.3$ mm and $\sigma_y = 1.8$ mm as outlined in section 2.3.3. The measureable signal for a given OSLD and beam size is calculated by averaging a two-dimensional Gaussian, with a given spread and impinging somewhere on the OSLD, over the OSLD surface. The lowest and highest measureable signals, due to averaging effects for a given OSLD and beam size, occur when the beam hits the corner and the center of the OSLD, respectively. These two limits outline the hatched area in figure 5. As the signal averaging changes with the position of the beam center relative to the OSLD, the dotted lines in figure 5 denote the mean value of all signal

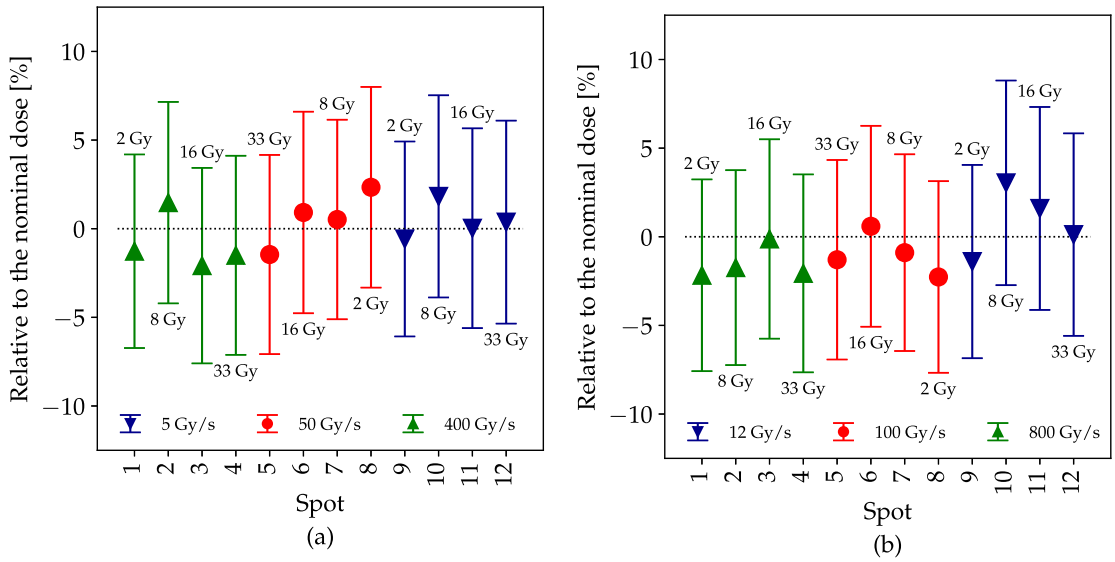

Figure 6. Measured OSLD doses using setup A for the 12 locations in two different frame configurations (a) and (b), with the nominal dose to each vial written next to the data point. The dose deviation of the OSLD is calculated relative to Faraday cup derived dose.

averages for a given OSLD size caused by the different beam spot centers over the OSLD. The average size of the 72 OSLDs used for the six irradiation of the 9000 Gy s^{-1} beam was found to be (1.2 ± 0.2) mm. The two vertical dashed lines represent the range corresponding to the two standard deviations around the mean OSLD size.

The signal averaging of the wider (1–1000) Gy s^{-1} beam is overall small for the relevant OSLD sizes, provided the beam spot center impinges on an OSLD. Nevertheless, as the OSLDs are immersed in the water-filled vials or cylinders, the beam center could miss the OSLD causing a larger averaging and a smaller evaluated dose.

The signal averaging of the narrow 9000 Gy s^{-1} beam defined in section 2.1 may cause the dose to be severely underestimated given the used OSLD sizes. In particular, the dose may be underestimated more than 10%, if the 9000 Gy s^{-1} beam is centered over the corner of a quadratic 1.40 mm OSLD—or much more if the OSLD is larger or the beam hits in-between OSLDs. Similarly, the dose measured in the 3800 Gy s^{-1} beam is to be underestimated by a few percent.

Nonetheless, the calculations in figure 5 show that 0.75 mm wide OSLDs placed tightly in a grid can be used to measure the dose of the narrow 9000 Gy s^{-1} pencil beam with at most 5% dose underestimation due to the averaging over the OSLD.

3.2. Dose measurements with OSLDs

3.2.1. Results for setup A: water-filled tubes

Figure 6 shows two examples of the results for frames accommodating vials with OSLDs, as shown in figure 1(b), where the vials were irradiated with several doses and dose rates. The dose measured with the OSLDs is plotted as the deviation relative to the dose derived from the Faraday cup measurement and shown above or below each data point. The irradiations of the remaining four frames are included in supplementary section A (available online at stacks.iop.org/PMB/66/085003/mmedia).

3.2.2. Results for setup B: water-filled cylinders

The results of the OSLDs irradiated in the water-filled cylinders constituting setup B, as outlined in section 2.3.2, are shown in figure 7. The figure shows the OSLD measured doses relative to the Faraday cup derived doses for two irradiations with three dose. Whilst the average of the front, center, and back OSLD doses would provide information about the dose delivered to biological samples placed in the water-filled cylinder, figure 7 shows the dose of the front OSLD nearest the nozzle as the dose varies through the cylinder. The OSLD dose is shown relative to the calculated dose to the cylinder front based on the Faraday cup measurement. The irradiation with a 3800 Gy s^{-1} pencil beam is included in supplementary section B.

3.2.3. Results for setup C: Grid OSLD measurements

Two measurements with the OSLD grid are shown in figure 8, where the edges of the irradiated OSLDs are delineated with black lines. The vertices of the quadrilateral OSLDs are estimated from a photo and extracted using a software script. A Gaussian function was fitted to each set of measured doses following the minimization procedure in section 2.3.3. The best fitting Gaussian is plotted over the outlined OSLDs in figure 8 with dashed

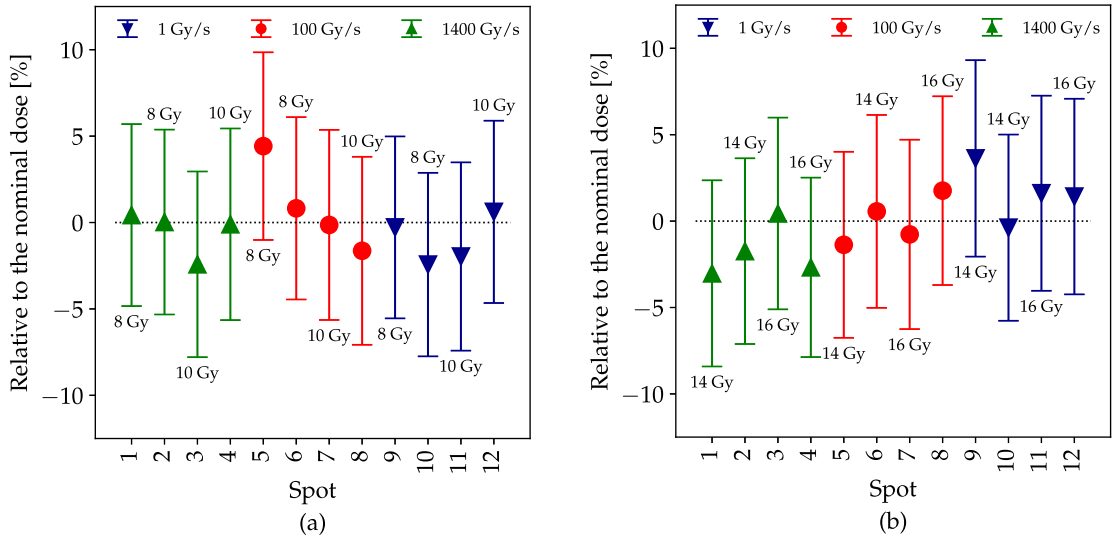

Figure 7. Measured OSLD doses using setup B for two irradiations (a) and (b) with the nominal dose to each vial written next to the data point. The dose deviation of the OSLD is calculated relative to Faraday cup derived dose.

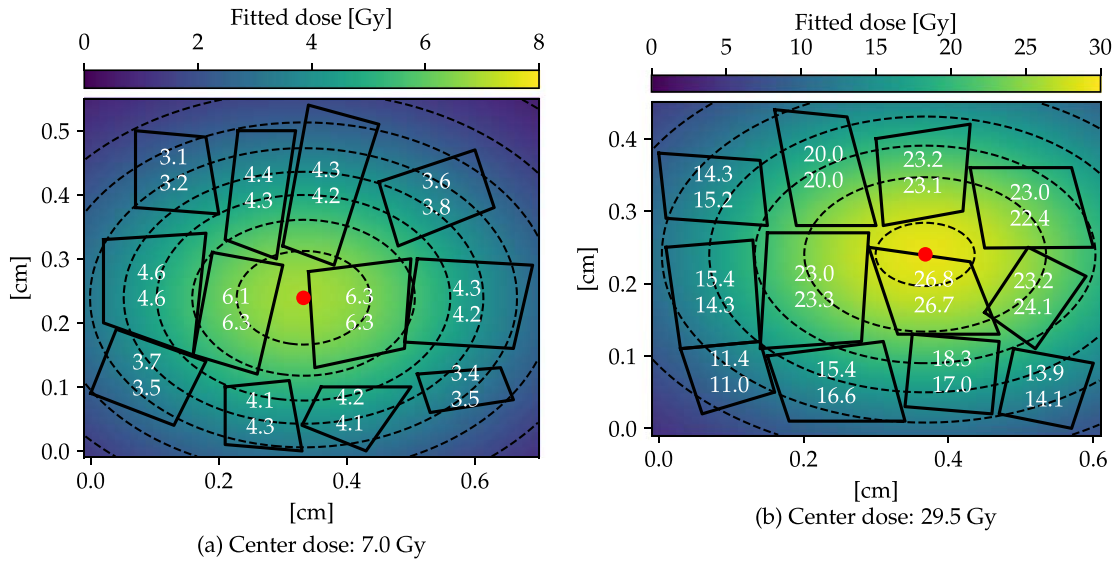

Figure 8. The OSLDs outlined with black, solid lines with the pencil beam aimed at the grid center. The upper number in each OSLD shows the measured dose in units of Gy, whereas the lower number is the dose in Gy to the OSLD evaluated with the best Gaussian fit. The interpolated dose at the center of the Gaussian is given below each figure as the dose to the center. (a) Shows the result for irradiation with a nominal 7.6 Gy dose and (b) with 31.7 Gy.

contour lines and a red circle as center with the dose given by the colorbar. The measured dose and the dose obtained from evaluating the resulting Gaussian function over each OSLD are given as the upper and lower number, respectively, in each delineated OSLD in units of Gy. The estimated doses from the Gaussian function fits in figures 8(a) and (b) were 7.0 Gy and 29.5 Gy, respectively, as given in the caption of each subfigure. These estimations are both about 8% lower than the nominal irradiation doses of 7.6 Gy and 31.7 Gy, respectively, derived from Faraday cup measurements. Four more OSLD grids were irradiated with the 9000 Gy s^{-1} pencil beam and included in supplementary section C.

The underestimated doses reflect the signal averaging arising from measurements with $>1\,mm^2$ sized OSLDs which, furthermore, are slightly misaligned in the grid: the expected signal averaging for the 9000 Gy s^{-1} beam and $>1\,mm^2$ OSLD is from figure 5 expected to be of the order (2−10)%. The underestimation due to the signal averaging, however, was calculated under the assumption of a tightly packed OSLD grid where the beam center would impinge directly on an OSLD. Both fits in figure 8 could indicate that the beam was centered between the OSLDs, which consequently would cause a dose underestimation larger than 10%. Hence, the

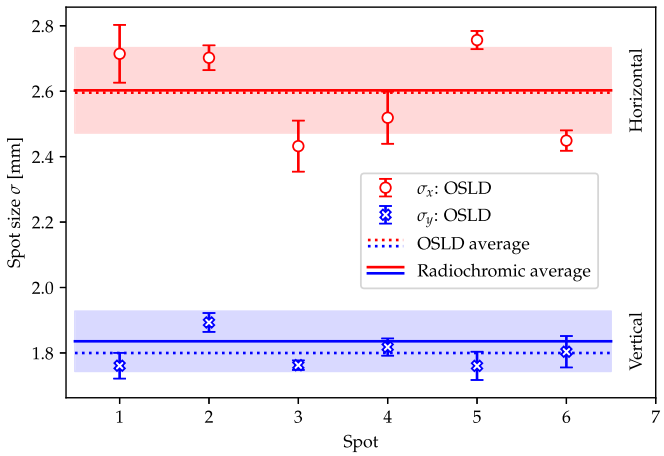

Figure 9. The 9000 Gy s^{-1} pencil beam spot spread σ obtained from the OSLD grid measurements by fitting a double Gaussian to the OSLD. The dotted and solid lines show the mean of the OSLD and radiochromic spot measurements, respectively. The filled areas show the ranges covered by two standard deviations of the radiochromic measurements around its mean.

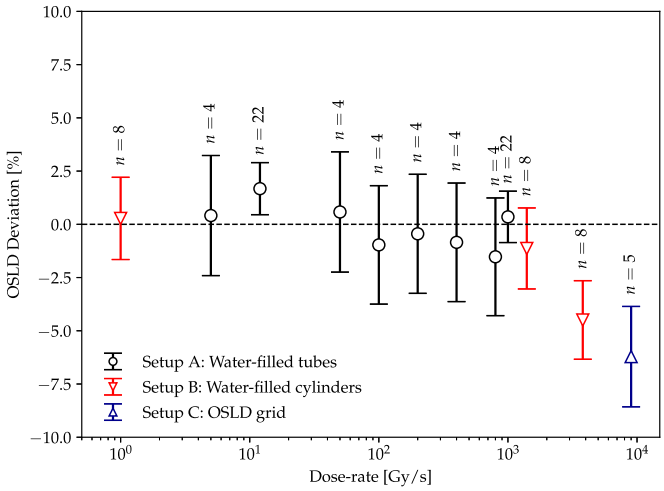

Figure 10. The deviation of the OSLD measured doses relative to the nominal dose as a function of the dose rate for the three methods A, B, and C. The number of aggregated data points for each dose rate is given above each marker. The decreasing response above 1000 Gy s^{-1} is due to signal averaging of the narrow pencil beam over the OSLDs.

underestimated dose evaluations are attributed to the averaging of the narrow pencil beam over the OSLDs rather than a dose rate dependency of the OSL material itself.

3.2.4. OSLD spot size measurement

The fit of a Gaussian function to the OSLD doses in figure 8 furthermore provides information about the spread of the spot sizes at 9000 Gy s^{-1} for the six delivered spots. The spot sizes obtained from the minimizations in the horizontal (x) and vertical (y) directions are plotted in figure 9.

The spot spreads measured with the OSLDs are in agreement with radiochromic film derived spot sizes within the uncertainties. The biggest discrepancy is observed for spot five with a 6% deviation relative to the mean of the radiochromic film measurements. The mean values of the OSLD derived spot sizes were $\sigma_x = (2.6 \pm 0.1)$ mm and $\sigma_y = (1.8 \pm 0.1)$ mm for the 9000 Gy s^{-1} pencil beam, in agreement with the radiochromic film measurements, which demonstrates the use of OSLDs to extract the beam spot size even for small pencil beams.

3.3. OSL dose measurements and dose rate dependency

The OSLD measurements for all doses and dose rates are compiled in figure 10, where the OSLD response is plotted as the deviation relative to the nominal dose as a function of the dose rate. The results are obtained using the three different measurement methods outlined in section 2.3, where the measurements for each dose rate have been averaged.

The ($n = 76$) OSLD doses for (1–1000) Gy s^{-1} have an average discrepancy of −0.1%, whereas the average deviation at 1000 Gy s^{-1} ($n = 22$) amounts to +0.4%. The −4.5% OSLD deviation at 3800 Gy s^{-1} is due to the signal averaging of the narrow pencil beam as demonstrated in section 3.1.4. The dose corrected with the Gaussian fits to the OSLD grid for the 9000 Gy s^{-1} beam deviates with −6.2% ($n = 5$), which is to be regarded as the best correction given the >1 mm^2 OSLDs and the misaligned grids.

The methods of using OSLDs in vials, cylinders, and distributing OSLDs in a grid have shown to be feasible for dosimetry in FLASH relevant proton beams. The use of 0.75 mm wide OSLDs placed tightly, or even overlapping, would decrease the signal averaging in the 3800 and 9000 Gy s^{-1} beams to a level within the experimental uncertainties.

4. Conclusion

Al_2O_3:C OSL were investigated in a pencil proton beam for a wide range of dose rates up to 9000 Gy s^{-1}, which corresponds to an instantaneous dose rate about 150 kGy s^{-1} within each pulse. The OSL calibration curve was established for the range (3–33) Gy. The luminescence fading was found to be less than 1.8% over a 3-week period. The signal averaging of the pencil beams over the OSLDs was mapped for a range of OSLD sizes and two pencil beam sizes, mimicking the experimentally used beams, to separate any dose-underestimation due to signal averaging from a present dose rate effect. The signal averaging of the (1–1000) Gy s^{-1} beam was found to be negligible for a 1 mm^2 OSLD but to constitute up to 10% in the narrow 9000 Gy s^{-1} beam and larger if the beam center does not impinge on an OSLD. The OSLDs were found to be dose rate independent. The observed signal averaging in the pencil beams above 1000 Gy s^{-1} can be remedied with smaller OSLDs.

The setups A and B with OSLD in vials and cylinders, respectively, to support irradiation of biological samples, were demonstrated to be on average within 2% of the nominal dose below 1000 Gy s^{-1}. A new technique (Setup C) to measure narrow pencil beams, using OSLDs in a grid, was demonstrated to correct the signal averaged dose slightly, and to extract the beam spot size with an average <1% deviation relative to radiochromic film measurements. Overall, it was demonstrated that Al_2O_3:C OSL can provide precise dosimetry to support radiobiological experiments in proton FLASH therapy experiments.

Acknowledgments

The authors thank Martina Egloff and Benno Rohrer for their support in the experimental setup and preparation of the instrumentation. The Risø TL/OSL-DA-20 reader (DTU Nutech, Denmark) was acquired with partial support from the Swiss National Science Foundation (R'Equip project 206021_177028). The work was partially supported by the Swiss National Science Foundation (grant CRSK-2_190663).

ORCID iDs

Jeppe Brage Christensen https://orcid.org/0000-0002-6894-381X
Konrad Pawel Nesteruk https://orcid.org/0000-0002-7482-2264
Serena Psoroulas https://orcid.org/0000-0001-7576-3238
Eduardo G Yukihara https://orcid.org/0000-0002-4615-6698

References

Akselrod M S, Agersnap Larsen N and McKeever S W S 2000 A procedure for the distinction between static and dynamic radiation exposures of personal radiation badges using pulsed optically stimulated luminescence *Radiat. Meas.* **32** 215–25

Akselrod M S, Bøtter-Jensen L and McKeever S W S 2007 Optically stimulated luminescence and its use in medical dosimetry *Radiat. Meas.* **41** S78–99

Beyreuther E, Brand M, Hans S, Hideghéty K, Karsch L, Leßmann E, Schürer M, Szabó E R and Pawelke J 2019 Feasibility of proton FLASH effect tested by zebrafish embryo irradiation *Radiother. Oncol.* **139** 46–50

Bourhis J *et al* 2019a Clinical translation of FLASH radiotherapy: why and how? *Radiother. Oncol.* **139** 11–7

Bourhis J *et al* 2019b Treatment of a first patient with FLASH-radiotherapy *Radiother. Oncol.* **139** 18–22

Buonanno M, Grilj V and Brenner D J 2019 Biological effects in normal cells exposed to FLASH dose rate protons *Radiother. Oncol.* **139** 51–5

Casey K E, Alvarez P, Kry S F, Howell R M, Lawyer A and Followill D 2013 Development and implementation of a remote audit tool for high dose rate (HDR) Ir-192 brachytherapy using optically stimulated luminescence dosimetry *Med. Phys.* **40** 112102–8

Chen R and Leung P L 2001a Dose dependence and dose-rate dependence of the optically stimulated luminescence signal *J. Appl. Phys.* **89** 259–63

Chen R and Leung P L 2001b Nonlinear dose dependence and dose-rate dependence of optically stimulated luminescence and thermoluminescence *Radiat. Meas.* **33** 475–81

Christensen J B, Almhagen E, Stolarczyk L, Liszka M, Hernandez G G, Bassler N, Nørrevang O and Vestergaard A 2020a Mapping initial and general recombination in scanning proton pencil beams *Phys. Med. Biol.* **65** 115003

Christensen J B, Vestergaard A and Andersen C E 2020b Using a small-core graphite calorimeter for dosimetry and scintillator quenching corrections in a therapeutic proton beam *Phys. Med. Biol.* **65** 215023
Darafsheh A, Hao Y, Zwart T, Wagner M, Catanzano D, Williamson J F, Knutson N, Sun B, Mutic S and Zhao T 2020 Feasibility of proton FLASH irradiation using a synchrocyclotron for preclinical studies *Med. Phys.* **47** 4348–55
Diffenderfer E S *et al* 2020 Design, implementation, and *in vivo* validation of a novel proton FLASH radiation therapy system *Int. J. Radiat. Oncol. Biol. Phys.* **106** 440–8
Esplen N M, Mendonca M S and Bazalova-Carter M 2020 Physics and biology of ultrahigh dose-rate (FLASH) radiotherapy: a topical review *Phys. Med. Biol.* **65** 23TR03
Favaudon V *et al* 2014 Ultrahigh dose-rate FLASH irradiation increases the differential response between normal and tumor tissue in mice *Sci. Transl. Med.* **6** 245ra93–ra93ra93
Gomà C, Lorentini S, Meer D and Safai S 2014 Proton beam monitor chamber calibration *Phys. Med. Biol.* **59** 4961–71
Hornsey S and Alper T 1966 Unexpected dose-rate effect in the killing of mice by radiation *Nature* **210** 212–3
Jaccard M, Petersson K, Buchillier T, Germond J-F, Durán M T, Vozenin M-C, Bourhis J, Bochud F O and Bailat C 2017 High dose-per-pulse electron beam dosimetry: usability and dose-rate independence of EBT3 Gafchromic films *Med. Phys.* **44** 725–35
Jursinic P A 2007 Characterization of optically stimulated luminescent dosimeters, OSLDs, for clinical dosimetric measurements *Med. Phys.* **34** 4594–604
Karsch L, Beyreuther E, Burris-Mog T, Kraft S, Richter C and Zeil K 2012 Dose rate dependence for different dosimeters and detectors: TLD, OSL, EBT films, and diamond detectors *Med. Phys.* **5** 2447–55
Kry S F *et al* 2020 AAPM TG 191 clinical use of luminescent dosimeters: TLDs and OSLDs *Med. Phys.* **47** e19–51
Lempart M, Blad B, Adrian G, Bäck S, Knöös T, Ceberg C and Petersson K 2019 Modifying a clinical linear accelerator for delivery of ultra-high dose rate irradiation *Radiother. Oncol.* **139** 40–5
Lin S, Boehringer T, Coray A, Grossmann M and Pedroni E 2009 More than 10 years experience of beam monitoring with the Gantry 1 spot scanning proton therapy facility at PSI *Med. Phys.* **36** 5331–40
Lye J *et al* 2014 Remote auditing of radiotherapy facilities using optically stimulated luminescence dosimeters *Med. Phys.* **41** 032102
Mijnheer B, Beddar S, Izewska J and Reft C 2013 *In vivo* dosimetry in external beam radiotherapy *Med. Phys.* **40** 070903
Nesteruk K, Togno M, Grossmann M, Lomax T, Weber D, Schippers M, Safai S, Meer D and Psoroulas S 2020 Commissioning of a clinical pencil beam scanning proton therapy unit for ultrahigh dose rates (FLASH) *Med. Phys.* arXiv:2101.01770 (Unpublished)
Newville M, Stensitzki T, Allen D B, Rawlik M, Ingargiola A and Nelson A 2016 LMFIT: non-linear least-square minimization and curve-fitting for python ascl ascl: 1606.014 (http://doi.org/10.5281/zenodo.11813)
Patriarca A *et al* 2018 Experimental set-up for FLASH proton irradiation of small animals using a clinical system *Int. J. Radiat. Oncol. Biol. Phys.* **102** 619–26
Sawakuchi G O, Sahoo N, Gasparian P B R, Rodriguez M G, Archambault L, Titt U and Yukihara E G 2010 Determination of average LET of therapeutic proton beams using Al_2O_3:C optically stimulated luminescence (OSL) detectors *Phys. Med. Biol.* **55** 4963–76
Town C D 1967 Effect of high dose rates on survival of mammalian cells *Nature* **215** 847–8
Vozenin M C *et al* 2019 The advantage of FLASH radiotherapy confirmed in mini-pig and cat-cancer patients *Clin. Cancer Res.* **25** 35–42
Wesolowska P E, Cole A, Santos T, Bokulic T, Kazantsev P and Izewska J 2017 Characterization of three solid state dosimetry systems for use in high energy photon dosimetry audits in radiotherapy *Radiat. Meas.* **106** 556–62
Winterhalter C *et al* 2018 Validating a Monte Carlo approach to absolute dose quality assurance for proton pencil beam scanning *Phys. Med. Biol.* **63** 175001
Yukihara E G, Doull B A, Ahmed M F, Brons S, Tessonnier T, Jäkel O and Greilich S 2015 Time-resolved optically stimulated luminescence of Al_2O_3:C for ion beam therapy dosimetry *Phys. Med. Biol.* **60** 6613–38
Yukihara E G and McKeever S W S 2006 Ionization density dependence of the optically and thermally stimulated luminescence from Al_2O_3:C *Radiat. Prot. Dosim.* **119** 206–17
Yukihara E G and McKeever S W S 2008 Optically stimulated luminescence (OSL) dosimetry in medicine *Phys. Med. Biol.* **53** R351–79
Yukihara E G, Yoshimura E M, Lindstrom T D, Ahmad S, Taylor K K and Mardirossian G 2005 High-precision dosimetry for radiotherapy using the optically stimulated luminescence technique and thin Al_2O_3:C dosimeters *Phys. Med. Biol.* **50** 5619–28